The International Journal of Advanced Manufacturing Technology
https://doi.org/10.1007/s00170-023-11578-9

ORIGINAL ARTICLE

Influence of the hydraulic press system on advanced high-strength steel formability

Edimar de Lima[1] · Murilo do Nascimento Cruz[1] · Ravilson Antonio Chemin Filho[1] · Chetan P. Nikhare[2] · Paulo Victor Prestes Marcondes[1]

Received: 13 March 2023 / Accepted: 10 May 2023

Abstract
In sheet-forming operations, it has been sought to always obtain the maximum elongation of the material without the occurrence of defects, a condition that is of fundamental importance to know the performance of the sheet metal in industrial processes. In view of this need, the FLCs (forming limit curves) of the used metal sheets are determined, which provide an excellent condition for the evaluation of the material stamping limit. Deformation levels lower than FLC, considering a safety margin, are considered satisfactory in industrial operations. Based on this, the objective of this work was the adequacy of a test machine and the development of a method to obtain the FLC of sheet metal at the beginning of the material's bonding, thus seeking a more precise result of the formability of the main steels used in the industry, advanced high strength steels. For this, an initial analysis of the hydraulic press was carried out where, taking advantage of the displacement and oil pressure sensors present, a new control program was determined in the PLC (programmable logic controller), to parameterize the points that precede the rupture of the sheet during the stamping test. Under these conditions, the FLC of the dual-phase steel DP600 was determined until its rupture and, later, until the point of its beginning, which allowed the definition of the real limit of formability of this material. In addition to the conclusion regarding the behavior of the material, considering the industrial processes, the results obtained also allow the determination of set points of machines more adequate to the limits of deformation of the sheet metal used. The FLC presented a variation, characterized by a small increase in the formability limit for the tests with hydraulic press temperature control conditions. The results highlighted higher temperatures on the pump, followed by the distributing block and the pressure sensor, concluding that the major influence critical point on the FLC result was the hydraulic pump.

Keywords Temperature · Blank holder force · Forming limit curve · DP600

1 Introduction

There is always a search for new methods to supply the needs for products with more efficiency in the automotive industry, the improvement in bodywork corresponds to improvements in studies for three different sections: AHSS steels [1–7], processing, and design. These lines of research are directly impacted by more advanced analysis methods for the material nature of stamping, being Nakazima the most highlighted test which has the purpose to compose the forming limit curves for sheet metals.

A typical and precise manner to predict the maximum formability of sheet metal is the forming limit curve (FLC). Developed by authors such as Keeler [8], Goodwin [9], and Woodthorpe et al. [10], it has been one of the main important devices for many authors for different meanings. Min et al. [11] disposed of a technique that the appearance of localized cracks through a transition in the curvature of the sheet metal surface. Affronti and Merklein [12] had their study on a sheet metal failure analysis in different cases of stress measured at the material surface, with Nakazima tests and the forming limit curve data, while Iquilio et al. [13] developed an empirical process for obtaining the sheet metal FLC with digital image correlation (DIC) and an optical technique, granting a more precise measurement on points

✉ Chetan P. Nikhare
cpn10@psu.edu

[1] Mechanical Engineering Department, Federal University of Paraná, Curitiba, PR, Brazil

[2] Mechanical Engineering Department, the Pennsylvania State University, Erie, PA, USA

Published online: 16 May 2023

throughout the sample surface for deformation and displacement analysis. Other mentions of different studies that required FLC and Nakazima stamping tests: Schmid et al. [6] discussed failure behavior in the mechanical forming process, and Barlo et al. [7] had a non-linear FLC model and traditional FLC research. Shinmiya et al. [14] granted failure and/or bending cracks on different flexibility sheet metal surface detection possibilities using the FLC. Norz and Volk [15] used the traditional Nakazima test to assess the model developed by Jocham et al. [16], having the resulting curves compared.

An important way to validate the efficiency of sheet metal in stamping is through studies regarding the influence of tool variants on its forming process, as analyzed by Chemin et al. [17] and Lajarin et al. [18]. Thus, a better knowledge surrounding stampability characteristics of sheet metal and tool variants is enabling design execution in less time, in a more precise and efficient manner in terms of used raw material. This advancement is fundamentally due to studies made focusing on the evaluation of tool and formability limits of sheet metal; these two main parameters determine the stamping operation efficiency. It is important to describe that the lubricant type is also a parameter that can improve the sheet metal formability, as shown by Tigrinho et al. [19], but it was not considered a main objective for this work.

The research was an experimental work, which utilized a sheet metal stamping tool with a blank holder force setting, used by Chemin et al. [17] and Tigrinho et al. [20] having the hydraulic press programmed for stopping during the test on the sheet metal necking point. The necking point is a crucial factor that emphasizes the reliability of an obtained FLC, Paul [21] illustrates the strain versus stress difference from diffuse to localized necking. Localized necking is mostly in the diffuse necking zone and harder to acquire the starting point, Paul [22] brings FLC near this point to a safe level of strain analysis, and Paul [23] shows a significant influence of material *r*-value on this factor.

2 Methodology

Initially, the hydraulic press was studied to verify its functioning, with sensors and data acquisition software. The press works with a double activation, which means the die and hemispheric punch are controlled by independent hydraulic pistons, originally activated by buttons on the press panel. There is a pressure gauge for the blank holder line, establishing the force. A pressure transducer tracks the punch-actuating piston's pressure. A linear encoder which tracks the punch displacement is also part of the set. To track all these sensors and valve actuation, the press has a PLC.

The software control records the sensors' values in 100-ms intervals. The utilized tool was a modified equipment from Chemin et al. [17], which possesses a hemispherical punch of 50 mm radius, straight die without draw-bead. This was tested by the author, and by applying 784.5 kN, it obtained similar results as to trials with draw-bead, therefore discarding the need for it.

DP600 was used for the procedure, produced, and supplied by Usiminas-MG, with 2.0 mm thickness, following the properties in Table 1. Among the AHSS (advanced high strength steel) focused on many studies, there are a few who mentions DP600 steel, such as Huh [24], Curtze [25], Farabi [26] Uthaisangsuk [27], Kim S. B. [28], Nikhare [29], and Bornancin [30].

The Nakazima tests (Fig. 1) predict a total of eighteen test specimens as detailed on ISO 12004-2 [31]; however, eight specimens were utilized, an amount considered suitable for the desired purpose. These specimens were defined with measures of 25mm, 50mm, 75mm 100mm, 120mm, 150mm,175mm, and 200mm, all cut by guillotine with 200mm width (Fig. 2).

Through screen printing, the test specimen had a circular grid printing on its surface, intended to measure the deformation suffered by the material after the forming process. Using only the paint from the screen-printing process, vinyl type black color, was not enough for an efficient marking, because the test specimen surface does not adhere to this paint easily. To solve this issue, nitric acid paint was added, a 10% ratio of the paint volume, making the adherence better to the material surface.

The first test taking the specimen to rupture with a blank holder force of 784.5 kN aimed to bring a FLC to validate the one obtained by Chemin et al. [17]. During the tests, punch displacement and hydraulic pressure were monitored to meet the machine parameters on the extreme point, corresponding to the material rupture.

With punch displacement and hydraulic press values, for the rupture point of DP600 steel, it was predicted that the necking point should represent values slightly lower. Consequently, it was experimentally worked with variation values for tests in which a 1% reduction for each test should represent satisfying values for visually detecting the necking point on the sheet. The software detects these established values and interrupts the test.

Table 1 Material mechanical properties (Usiminas-MG, 2019)

DP 600 STEEL	
Properties	Average value
YS (Mpa)	350
UTS (Mpa)	600

YS yield strength, *UTS* ultimate tensile strength

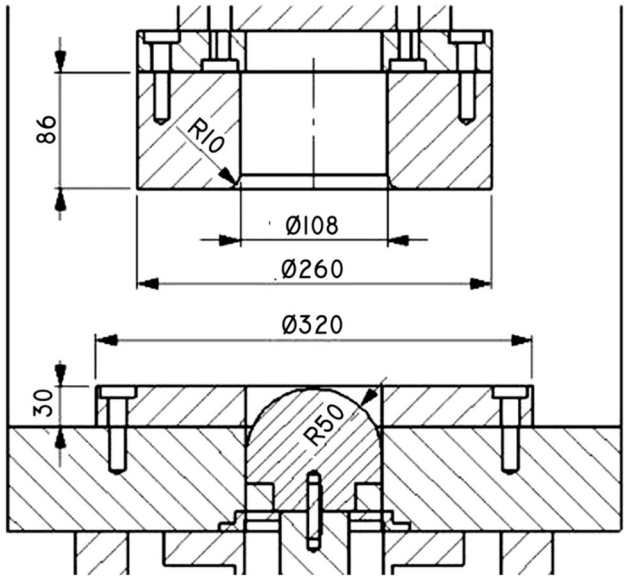

Fig. 1 Nakazima tool geometry for FLC determination

It was observed that some not monitored parameters could affect the tests, one of them being the hydraulic temperature of the machine which could interfere with the sensor reading. Therefore, new tests were carried out aiming to check if this temperature was really affecting the results.

Firstly, the machine temperature has been monitored in three measure points, considered more critical, the hydraulic pump, the entry block which distributes to the directional valves, and the hydraulic pressure gauge that sends the data to the PLC, shown in Fig. 3. It was necessary to check at which temperature these three points would stabilize; from that measure, there would be no major variation. By empirical means, it was attributed that by each 1 min, the temperature on these three points would stabilize.

New tests taking the specimens to rupture were conducted from the stabilized temperature, which means that the tests were starting on these conditions and would wait until the measured points would stabilize again for another test to be started. The test in these conditions was entitled "with temperature control," the objective was to verify if the press temperature would infer the FLC result until the rupture. Already "without temperature control" were the tests in which none of the original procedures was altered.

The reason why the pump, the distributing block, and the pressure gauge temperature were measured is because they correspond to the main components that integrate the hydraulic circuit of the press that powers the actuators, since the oil exit from the reservoir. Due to these components being metallic, the temperature measure on these points is simpler. Thus, the stamping efforts under the hydraulic system heating can be analyzed, which impacts the oil viscosity and consequently the sheet metal forming.

In all these tests, the temperatures of the pump, the distributing block, and the pressure gauge sensor were measured immediately before and after the test for a specimen, following the machine parameters obtained on the tests until rupture with controlled temperature, providing the machine control software with 95% pressure data and 98% of displacement value of the obtained values during the tests. These values were attributed based on the results of the tests previously described until rupture, which reported satisfying results on these percentages. Thus, the tests following the proposed methodology of stopping on the DP600 steel necking point were executed.

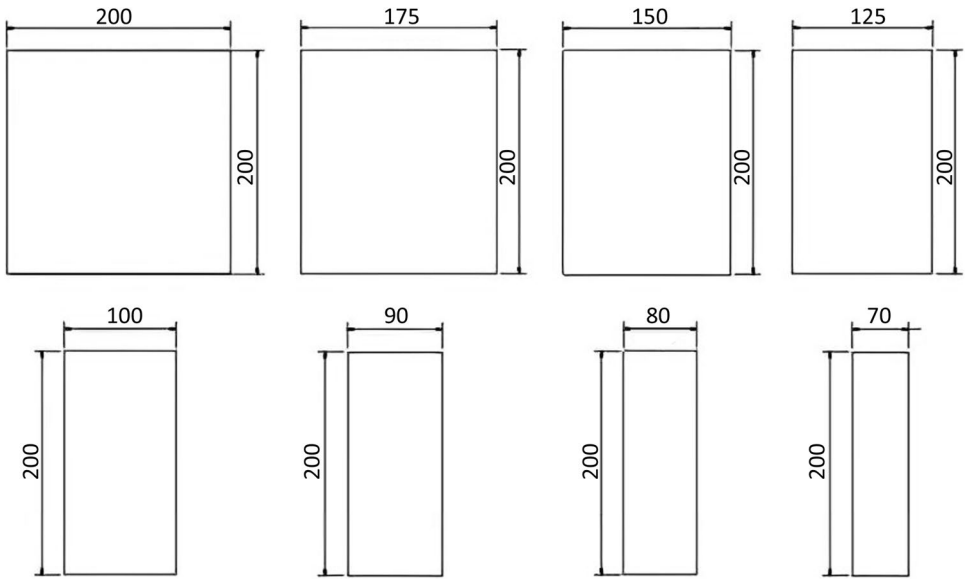

Fig. 2 Specimen geometries carried out on Nakazima's tests

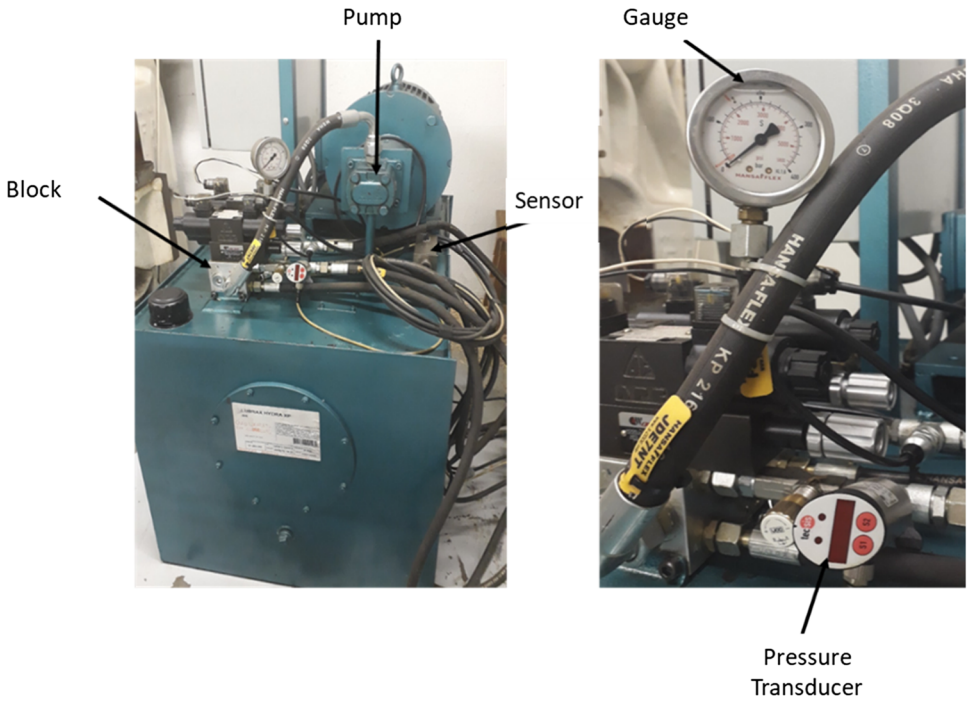

Fig. 3 Pressure gauge and transducer

3 Results and Discussion

The test's first step had the objective of identifying the thermic balance temperature of the pump, the distributing block, and the pressure gauge sensor, in other words, the main devices of the hydraulic machine power-generating unit. The plot represented in Fig. 4 shows the temperature variation on the pump, the block, and the gauge during the 60-min monitoring.

Notice that the pump temperature is superior to the sensor and the blocking temperature from the start until its stability. Still at the start, soon after the press is turned on, the pump temperature was already around 1° superior to the block and sensor temperature. During the measurement, it is observed that with the machine on however without the cylinder activation, the pump temperature constantly raises reaching a 5 °C value higher than the block and sensor temperature during the 60-min monitoring. It also noticed a gradual temperature increase, however highlighting that the pump presented higher temperature over the 60 min, taking approximately 4 min longer than the block and sensor to reach the stable thermic temperature. The sensor reported temperature stability before the other two devices, from the 41st minute of monitoring. The distributing block shows temperature stability from the 47th-minute monitoring, reaching a final balance temperature of 26 °C, the same value as the sensor. The pump's stable thermic temperature occurred after 50-min monitoring, being stable at 30 °C.

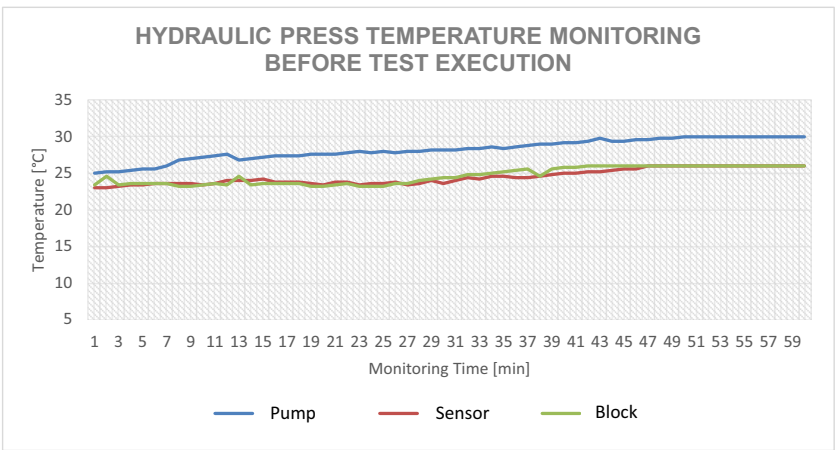

Fig. 4 Pump, sensor, and block temperature monitoring before test execution

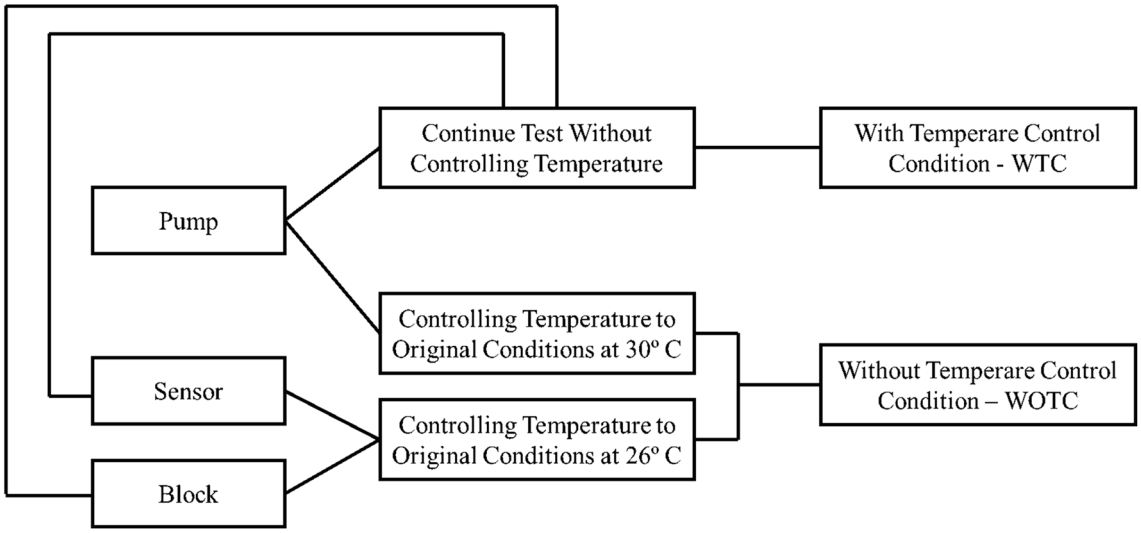

Fig. 5 Flowchart on tests conditions with and without temperature control conditions

Looking at this monitoring process, it was established the balance thermic temperatures necessary to start the tests on the hydraulic press, maintaining it for at least 50 min before starting any practical work. In this condition, the pump will reach 30°C while the pressure sensor and the distributing block will be at 26 °C. Starting the test on these device temperature conditions will eliminate any influence on the thermic variation which resulted from the initial phase of the equipment heating on the test results, as displayed in the flowchart in Fig. 5.

After reaching the machine thermic balance on the hydraulic unit devices (pump, block, and sensor), stamping tests were done with DP600 steel. For each test specimen tested, temperature measures were taken from the three hydraulic devices, immediately before and after the stamping process for each sample, presented in Fig. 6.

It is observed that without a temperature control configuration for the pump, the initial temperature varies between 46 and 50 °C. Also, for this analysis, the maximum temperature reached at the end of the tests was 80°C for the 200 × 200 mm specimen and for the 100 × 200 mm specimen, while the minimum final temperature was 75 °C, which characterizes a 5 °C variation between the maximum and the minimum final average temperature detected on the pump.

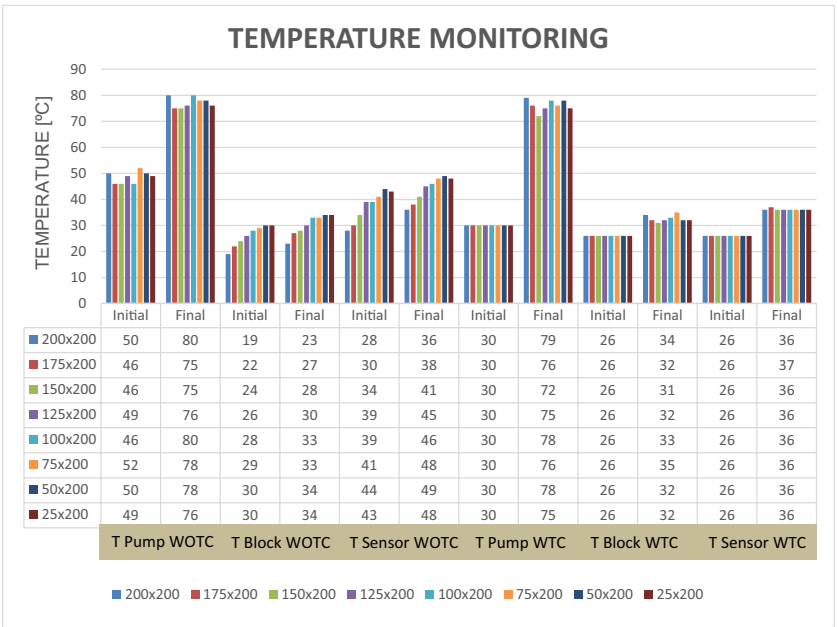

Fig. 6 Pump, block, and sensor temperature registered for each test start and ending with and without temperature control

Regarding the monitoring carried out on the distributing block on test conditions without temperature control, it is seen that the initial test temperature reached its minimum value for the specimen of 200 × 200 mm of 19 °C. The maximum final test temperature of 34 °C was identified for the smallest specimen tested: 50 × 200 mm and 25 × 200 mm. The block has shown a gradual increase, initial and final over the carrying of the tests. The temperature at the start of each test varied from 19 to 30 °C, while the temperature at the end of the tests went from 23 °C and reached 34 °C, considering that the tests were conducted for the specimens from the maximum width to the minimum width.

For the pressure sensor temperature monitoring, on test conditions without temperature control, the minimum and the maximum average value of the initial temperatures was obtained for the 200 × 200 mm and the 25 × 200 mm specimens respectively. The maximum average final temperature of the tests was achieved for the 25 × 200 mm specimen. The average initial test temperature was not lower than 28 °C nor higher than 43 °C, which characterizes a 17 °C variation from the first specimen test (200 × 200 mm) to the eighth specimen test (25 × 200 mm). The final test temperature also presented a gradual increase from the first specimen test (200 × 200 mm) to the last specimen test (25 × 200 mm), equivalent to 12°C. For the conducted tests without temperature control, it was registered the average time between each one of the 8 stamped test specimens as shown in Fig. 7.

The times shown in the plot correspond to the stamping start and end intervals of the sheet metal, when there was a temperature increase due to the activation of the hydraulic cylinder and later the interval of the removal and positioning of the next specimen, the latter a period of equipment cooling due to the deactivation of the hydraulic cylinder. The time difference between these test intervals registered on the plot is because all the specimen movement is manually made by the operator, not allowing for a precise pattern during the tests.

The curves shown in Fig. 6 represent the thermic variation on the hydraulic press devices. We also noticed that the pump reported higher temperatures than the sensor or the distributing block. Another important characteristic observed in the plot is that the pump thermic variation, on the interval between the tests, is highly steep during heating as much as in cooling. The average hydraulic pump heating and cooling rate was 0.47 °C/s and −0.57 °C/s respectively. The distributing block provided an average heating rate of 0.077 °C/s and an average cooling rate of −0.054 °C/s. The average heating and cooling rate of the pressure sensor was respectively 0.118 °C/s and −0.093 °C/s.

The temperatures reached on the hydraulic press devices, on "with temperature control" test condition, are been presented in Fig. 5. In this test condition, all the samples have been stamped with the same initial temperature, according to pre-determined values from Fig. 6 plot for the pump, the distributing block, and the hydraulic press sensor.

The initial pump test temperature, on the "with temperature control" condition, was 30 °C for all the test specimens, meaning that by the end of each test, the procedure was to wait for the device temperature to reach 30 °C again before starting a new stamping test. The final pump temperatures were once higher than the sensor and block final temperature. The maximum pump temperature registered, 79°C, occurred during the first specimen test (200 × 200 mm). It was observed a variation in the pump's final temperature between 72 and 79 °C and a variation of 7 °C between the minimum and the maximum values of the final temperature. This variation corresponds to a higher difference than in the test condition "without temperature control," which was 5 °C.

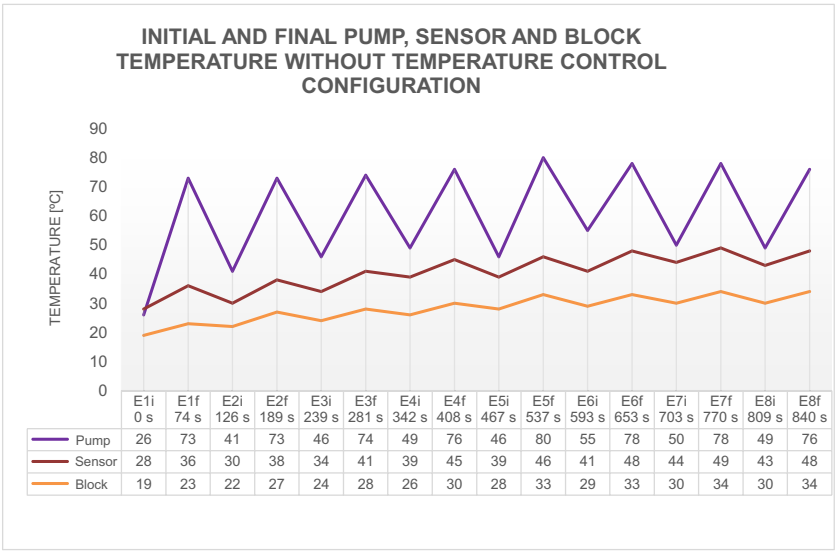

	E1i 0 s	E1f 74 s	E2i 126 s	E2f 189 s	E3i 239 s	E3f 281 s	E4i 342 s	E4f 408 s	E5i 467 s	E5f 537 s	E6i 593 s	E6f 653 s	E7i 703 s	E7f 770 s	E8i 809 s	E8f 840 s
Pump	26	73	41	73	46	74	49	76	46	80	55	78	50	78	49	76
Sensor	28	36	30	38	34	41	39	45	39	46	41	48	44	49	43	48
Block	19	23	22	27	24	28	26	30	28	33	29	33	30	34	30	34

Fig. 7 Pump, block, and sensor temperature register during tests for "without temperature control condition"

For the distributing block, for which the stable thermic temperature was 26 °C, it was noticed that the minimum final temperature of 31 °C was identified on the third specimen test (150 × 200 mm), while the maximum final temperature was registered for a 75 × 200 mm specimen test, reaching 35 °C that determined a limit difference of 4 °C.

The pressure sensor temperature variations on the "with temperature control" condition were the lowest registered during the tests. Except for the specimen (175 × 200 mm), that reached 37 °C, all the remaining have elevated the sensor temperature from 26 to 36 °C.

The original circular grid mesh printed on the material samples was composed of 5-mm circles; these shapes became elliptical shapes after the test due to the material deformation. Following the Chemin 2013 [17] procedure, the largest ellipses on the strain area were measured representing the highest strains reached by the material to its necking or rupture. As the strain radial distance is symmetrical, the measure is done on the opposite side of the necking or rupture. Figure 8 shows the samples carried out until necking formation.

The major and minor axis of the ellipse, D_1 and D_2, provides the conventional strain e1 and e2 respectively through Eqs. (1) and (2):

$$e_1 = \frac{D_1 - D_0}{D_0} \tag{1}$$

$$e_2 = \frac{D_2 - D_0}{D_0} \tag{2}$$

D_0 is the original circular axis dimension. After that, the true strains were obtained through Eqs. (3) and (4):

$$\varepsilon_1 = \ln\left(e_1 + 1\right) \tag{3}$$

$$\varepsilon_2 = \ln\left(e_2 + 1\right) \tag{4}$$

Plotting ε_1 versus ε_2 values is how the FLC are obtained. Figure 9a shows a comparison between the FLC curves obtained to the rupture limit of the DP600 steel, with a blank holder load of 80 ton., with and without machine temperature control conditions. On stable machine temperature after 70 min, the FLC became equivalent to the curve obtained on the "without temperature control" test condition; it can be said that heating the system did not cause a variation in the press functioning conditions sufficiently enough, to the extent of determining a steel forming limit to its rupture. In the following tests, DP600 necking limit FLC curves were determined, as shown in Fig. 9b.

Stamping tests were made with 80 ton. on the blank holder, controlling the punch stopping point 5% less than the maximum hydraulic pressure limit and 2% less than the maximum punch displacement, based on studies done until the material rupture.

Figure 9b points to the reduction suffered on the DP600 steel FLC, when considering maximum deformation on the material necking limit, compared to the FLC obtained from the material rupture limit. This difference reached 0.05 larger deformation on plane stress state, a larger difference for elongation, and less for bi-axial deformation such as deep-drawing. It can be said that for the elongation state, there is a larger difference between the necking and rupture limit, and for deep drawing is the opposite, minor difference between the necking and rupture limit.

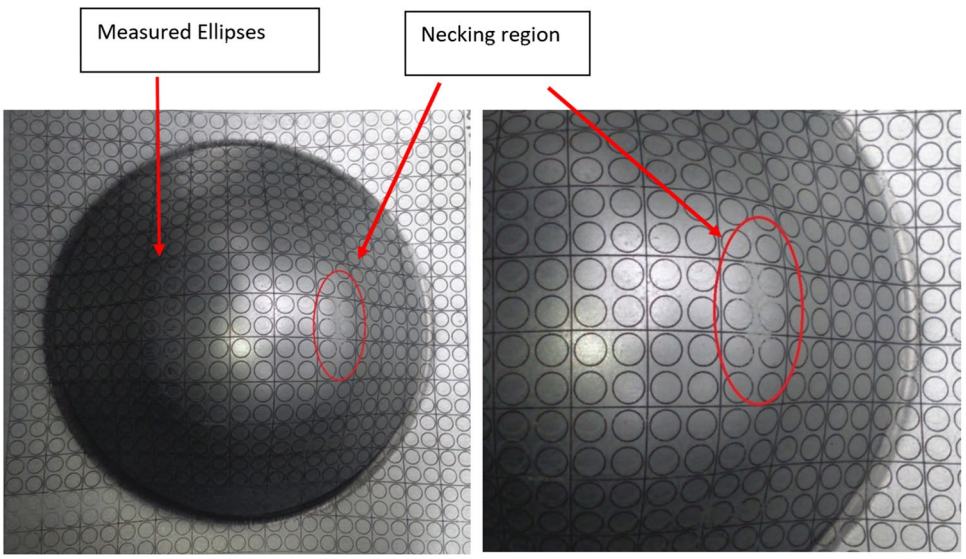

Fig. 8 Samples tested up to the onset of necking

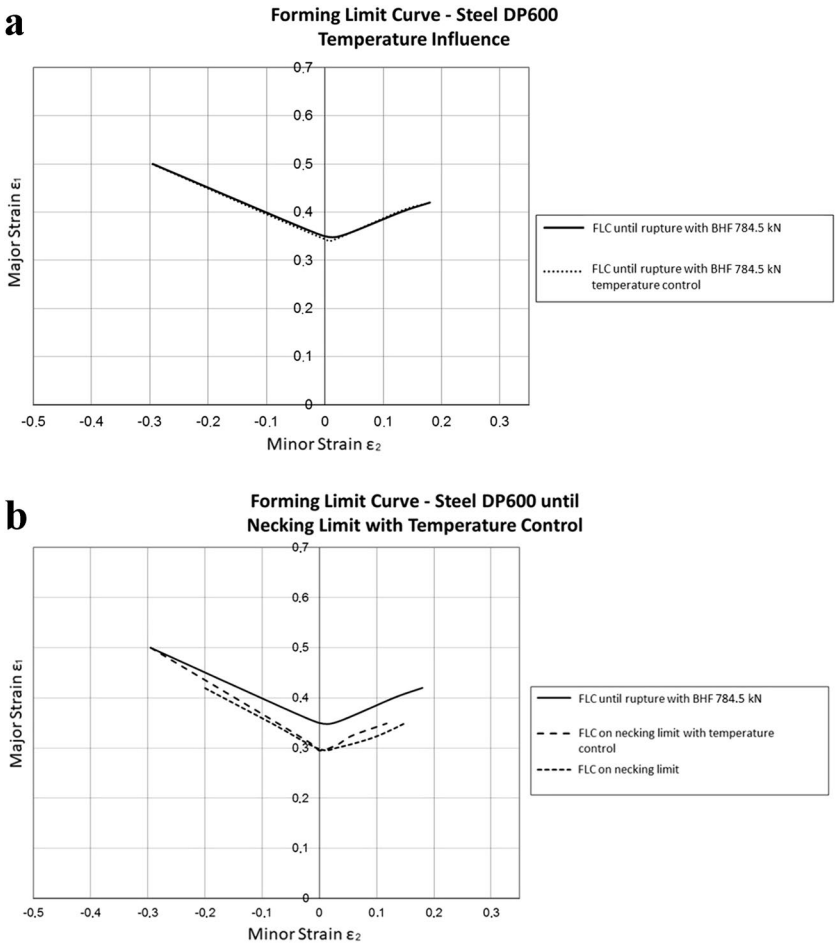

Fig. 9 Comparison obtained with and without temperature control **a** between the material rupture limit curves and **b** between the material necking limit curves

Analyzing Fig. 9b stamping tests until necking limits with and without temperature control, there is a slight variation between the curves. In the plane stress state, there is basically no difference between them; for the deep-drawing state, the difference was also low. For elongation, however, there was a steep difference, an order of 0.02 for the larger deformation.

This is justified because there is more hydraulic pressure on elongation when compared to deep drawing, thus having for elongation more blank holder action on the sheet flange, requiring more load for its formability. Therefore, during the elongation process, the influence on the oil viscosity is also higher due to the heating imposed on it, resulting in more variation in the FLC. For the tests done until rupture, the difference between the FLC with and without temperature control was insignificant, on account of the material already exceeding the necking limit reaching sheet metallurgical collapse, making imperceptible the machine oil viscosity influence on the forming limit of the DP600 steel.

4 Conclusion

The main conclusion of this work is that the temperature of the machine influences the sheet metal forming limit. The tests were conducted with the temperature control of the hydraulic press, showing a better formability limit of DP600 steel. The results presented above emphasize that after the press heating for stamping, until rupture tests carry off the DP600 steel with the temperature control condition, the resulting FLC showed a variation, which was characterized by a slight increase in the formability limit. Therefore, when the initial temperature is maintained at a fixed value, being that temperature beforehand established as the thermic stabilized temperature of the hydraulic system, the FLC reflected the higher limits. This improvement noticed on the FLC is due to the influence of the heat absorbed by the oil, which caused a variation of its properties, consequently leading the material to a higher deformation until it reached its programmed hydraulic pressure limit, which is derived from the steel necking limit analysis.

It is also important to notice that the pump is the component which has the highest oil temperature (Fig. 4) and shows the higher impact on temperature variation during the machine activation during the sheet metal forming (Fig. 6), concluding that the pump has the most impact on the hydraulic oil heating, and consequently on the temperature variations during the tests that affect the FLC.

The main point is the influence of the machine on the sheet metal forming process. It was inquired based on the test results that the higher temperatures reached were identified on the pump, followed by the sensor and the block. The critical point, with a major influence on the FLC result, was the hydraulic pump.

This highlights the inferring variables' influence on the equipment in the sheet-forming process, which in practice is not commonly observed in the industry. This means that studies on process factor influences can be of high relevance, especially for more efficient manufacturing designs offering better results, and the importance of improving machines for formability, controlling temperatures, and further variables that could directly interfere with the result, ensuring a better work process.

Availability of data and material Not applicable.

Code availability Not applicable.

Funding This research was funded by the Siderúrgica ArcelorMittal S/A (DP780 supply) and the CNPq (Brazil).

Declarations

Ethics approval Not applicable.

Consent to participate Not applicable.

Consent for publication Not applicable.

Conflict of interests The authors declare no competing interests.

References

1. Keeler S, Kimchi M (2015) Advanced high-strength steels application guidelines V5. WorldAutoSteel
2. Andrade SL, PEREIRA J, TAISS EUA (2000) O aço no automóvel do futuro: A estratégia da Usiminas. Contribuição técnica ao 55º Congresso Anual da ABM. Rio de Janeiro/RJ 55
3. Abeyrathna B, Rolfe B, Hodgson P, Weiss M (2016) A first step towards a simple in-line shape compensation routine for the roll forming of high strength steel. Int J Mater Form 9:423–434
4. Olavo, H (2017) (Porto Alegre). 37th S e N A F O R. Influência da geometria do quebra-rugas na factibilidade do processo de estampagem com base no Método dos Elementos Finitos: Influence of drawbead geometry on stamping feasibility based on Finite Elements Method. Disponível em: http://www.2017.senafor.com/conteudo/view?ID_CONTEUDO=442. Accessed 4 2017
5. Ke J, Liu Y, Zhu H, Zhang Z (2018) Formability of sheet metal flowing through drawbead–an experimental investigation. J Mater Process Technol 254:283–293
6. Schmid H, Hetz P, Merklein M (2019) Failure behavior of different sheet metals after passing a drawbead. Procedia Manuf 34:125–132
7. Barlo, A., Sigvant, M., & Endelt, B. (2019). On the failure prediction of dual-phase steel and aluminium alloys exposed to combined tension and bending. In IOP Conference Series: Materials Science and Engineering Vol. 651, No. 1, 012030 IOP Publishing
8. Keeler SP (1965) Determination of forming limits in automotive stampings (No. 650535). SAE technical paper
9. Goodwin GM (1968) Application of strain analysis to sheet metal forming problems in the press shop. SAE Trans:380–387
10. Woodthorpe J, Pearce R (1969) effect of R and N upon the forming limit diagrams of sheet steel. Sheet Metal Ind 46(12):1061–1067
11. Min J, Stoughton TB, Carsley JE, Lin J (2016) Compensation for process-dependent effects in the determination of localized necking limits. Int J Mech Sci 117:115–134
12. Emanuela A, Marion M (2017) Metallographic analysis of Nakajima tests for the evaluation of the failure developments. Procedia Eng 183:83–88
13. Iquilio RA, Cerda FC, Monsalve A, Guzmán CF, Yanez SJ, Pina JC et al (2019) Novel experimental method to determine the limit strain by means of thickness variation. Int J Mech Sci 153:208–218
14. Shinmiya, T., Fujii, Y., Yamasaki, Y., & Tamai, Y. (2019). Investigation of crack prediction method using limiting surface strain in high-strength steel sheets. In IOP Conference Series: Materials Science and Engineering Vol. 651, No. 1, 012065 IOP Publishing
15. Norz R, Volk W (2019) Investigation of non-proportional load paths by using a cruciform specimen in a conventional Nakajima test. In: IOP Conference Series: Materials Science and Engineering, vol 651, No. 1. IOP Publishing, p 012020
16. Jocham D, Gaber C, Böttcher O, Volk W (2015) Prediction of formability for multi-linear strain paths. Proc. Of FTF 2015:59–64
17. Chemin Filho RA, Valente Tigrinho LM, Barreto Neto RC, Marcondes PVP (2013) An experimental approach for blankholder force determination for DP600 with different material flow strain rates in the flange during stamping. Proc Inst Mech Eng B J Eng Manuf P I Mech Eng B-J Eng 227(3):417–422
18. Lajarin SF, Marcondes PV (2015) Influence of process and tool parameters on springback of high-strength steels. Proc Inst Mech Eng B J Eng Manuf P I Mech Eng B-J Eng 229(2):295–305
19. Tigrinho LMV, Santos RAD, Chemin Filho RA, Marcondes PVP (2008) Experimental investigation on the influence of the lubricant type in the punch stretching of extra deep-drawing steel. J Braz Soc Mech Sci Eng 30:290–294
20. Valente Tigrinho LM, Chemin Filho RA, Prestes Marcondes PV (2013) Fracture analysis approach of DP600 steel when subjected to different stress/strain states during deformation. Int J Adv Manuf Technol 69:1017–1024
21. Paul SK (2021) Controlling factors of forming limit curve: a review. Adv Indust Manuf Eng 2:100033
22. Paul SK (2016) Prediction of complete forming limit diagram from tensile properties of various steel sheets by a nonlinear regression based approach. J Manuf Process 23:192–200
23. Paul SK (2020) A critical review on hole expansion ratio. Materialia 9:100566
24. Huh H, Kim SB, Song JH, Lim JH (2008) Dynamic tensile characteristics of TRIP-type and DP-type steel sheets for an auto-body. Int J Mech Sci 50(5):918–931
25. Curtze S, Kuokkala VT, Hokka M, Peura P (2009) Deformation behavior of TRIP and DP steels in tension at different

temperatures over a wide range of strain rates. Mater Sci Eng A 507(1-2):124–131
26. Farabi N, Chen DL, Li J, Zhou Y, Dong SJ (2010) Microstructure and mechanical properties of laser welded DP600 steel joints. Mater Sci Eng A 527(4-5):1215–1222
27. Uthaisangsuk V, Prahl U, Bleck W (2011) Modelling of damage and failure in multiphase high strength DP and TRIP steels. Eng Frac Mech 78(3):469–486
28. Kim SB, Huh H, Bok HH, Moon MB (2011) Forming limit diagram of auto-body steel sheets for high-speed sheet metal forming. J Mater Process Technol 211(5):851–862
29. Nikhare C, Marcondes PV, Weiss M, Hodgson PD (2008) Experimental and numerical evaluation of forming and fracture behaviour of high strength steel. In: Proc. Of New Developments on Metallurgy and Applications of High Strength Steels. Buenos Aires, Argentina pp 26–28
30. De Araujo Bornancin RM, Nikhare CP, Marcondes PVP (2023) Numerical comparison of advanced high strength steels forming limit curve using Banabic and Nakazima tests. Int J Interact Des Manuf:1–10. https://doi.org/10.1007/s12008-023-01218-7
31. ISO (2008) Metallic materials-sheet and strip-determination of forming-limit curves-part 2: determination of forming-limit curves in the laboratory. ISO